

## **A BGO spectrometer for 200 – 1500 MeV photons**

M. Anghinolfi, M. Castoldi, P. Corvisiero, G. Gervino, L. Mazzaschi, V. Mokeev, G. Ricco, M. Ripani, M. Sanzone, M. Taiuti, A. Zucchiatti, N. Bianchi, E. De Sanctis, A. Ebolese, A. Fantoni, P. Levi Sandri, V. Lucherini, V. Muccifora, E. Polli, A.R. Reolon, P. Rossi

*Nuclear Instruments and Methods in Physics Research A317 (1992) 531-536*

## A BGO spectrometer for 200–1500 MeV photons

M. Anghinolfi, M. Castoldi, P. Corvisiero, G. Gervino <sup>1)</sup>, L. Mazzaschi, V. Mokeev <sup>2)</sup>, G. Ricco, M. Ripani, M. Sanzone, M. Taiuti and A. Zucchiatti

*Dipartimento di Fisica dell'Università e Sezione INFN, Via Dodecaneso 33, I-16146, Genova, Italy*

N. Bianchi, E. De Sanctis, A. Ebolese, A. Fantoni, P. Levi Sandri, V. Lucherini, V. Muccifora, E. Polli, A.R. Reolon and P. Rossi <sup>3)</sup>

*INFN-Laboratori Nazionali di Frascati, C.P. 13, I-00044 Frascati, Italy*

Received 21 October 1991 and in revised form 10 January 1992

A BGO spectrometer used at Frascati both as a monitor for a tagged-photon beam and as a photon spectrometer in a total photonuclear absorption experiment is described. Measured characteristics of the detector (response function, energy resolution, and tagged-bremsstrahlung spectra of energy up to 1.5 GeV) are shown, and compared to a Monte Carlo simulation.

### 1. Introduction

Crystals of bismuth-germanate  $\text{Bi}_4\text{Ge}_3\text{O}_{12}$  (BGO) are used or proposed as detectors on increasing number of electromagnetic calorimeters for their well known characteristics [1,2]: 1) short radiation length, 1.13 cm (to be compared with the 2.54 cm of NaI); 2) excellent energy resolution for intermediate and high photon energies; 3) good mechanical properties and 4) easiness of handling (non-hygroscopicity).

In this paper we report on a BGO spectrometer of original design (a cylindric BGO crystal surrounded by a NaI(Tl) anticoincidence shield) used on the 200–1500 MeV tagged photon beam produced at Frascati by the bremsstrahlung on a jet-target of the electrons circulating in the ADONE storage ring [3,4]. This detector has been designed both as a low intensity photon beam monitor and a photon spectrometer in the measurement of the tagger characteristics (energy calibration, efficiency and probability of tagging) [5], and as a spectrometer in a measurement of the total nuclear photoabsorption cross section on light nuclei performed with the transmission method [6].

Since in both cases the spectrometer must determine the energy of each single photon of the beam, particular care has been devoted while choosing the electronic components in order to guarantee good stability and linearity of the whole system still in presence of relatively high photon counting rate ( $N_\gamma \leq 10^4$   $\gamma/s$ ). In particular, this case has been found useful in the total photonuclear cross section measurement, where a very accurate determination of the number and energy of the photons reaching the spectrometer with the absorber in and out the beam is required [6].

In section 2 we discuss the main features of the spectrometer as well as the electronics scheme and the calibration procedure, while in section 3 we show the experimental response function, the energy resolution and a few measured bremsstrahlung spectra produced on a thin argon cluster-jet radiator together with Monte Carlo shower calculations.

### 2. Experimental setup

#### 2.1. The crystal spectrometer

The spectrometer, schematically shown in fig. 1, has been designed as a total absorption detector: running the EGS4 code with 1.5 GeV photons, a total length of 32 cm was found sufficient to longitudinally absorb more than 99% of the incoming energy. Moreover considering a 1.5 GeV monochromatic photon beam with a spot of 1 cm radius hitting a BGO cylinder 32

<sup>1)</sup> Permanent address: INFN-Sezione Torino, Via P. Giuria 1, I-10125 Torino.

<sup>2)</sup> Permanent address: Moscow University, Leninskye gory m.s.v., 119899 Moscow, Russia.

<sup>3)</sup> Permanent address: INFN-Sezione Sanità, Viale Regina Elena 299, I-00161 Roma.

cm long and 9.5 diameter, the absorbed energy spectrum has a FWHM of  $\approx 3\%$  intrinsic energy resolution, largely due to the lateral energy escapes.

Since at present it is technically impossible to produce a single BGO cylinder of such a dimensions without losing the crystal homogeneity, we designed the spectrometer as formed of four cylindrical sectors, each 8 cm long and 9.5 cm diameter, optically separated by thin aluminium walls. The lateral energy escape is absorbed by a 15 cm thick NaI annular ring, divided in three sectors (see fig. 1), which surround the inner BGO cylinders: if, for example, a 25 MeV anticoincidence threshold is used at  $E_\gamma = 1$  GeV, the calculated BGO's FWHM energy resolution drops to  $\approx 1.5\%$  with the detector efficiency lowered to  $\approx 50\%$ . As seen, the resolution and efficiency of such a spectrometer is strongly dependent upon the size of the BGO crystals and upon the threshold in the NaI anticoincidence shield; moreover, the real resolution is affected also by crystal nonuniformities which are difficult to model in any realistic way.

In order to keep the value of the resolution as close as possible to the calculated value, three couples of XP2012 photomultipliers were positioned at  $120^\circ$  on the lateral surface of each BGO. This configuration is a compromise between light collection, NaI anticoincidence geometrical efficiency, cost of electronics, and complexity.

Each of the three NaI anticoincidence sectors is seen on the rear by three Hamamatsu R1652 PMTs, being the NaI light collection less crucial than for BGO.

As already mentioned in the introduction, this spectrometer is directly exposed to the photon beam produced by the bremsstrahlung of electrons on a molecular jet of argon. High counting rate can, therefore, produce a non-negligible value of the anode current, which, on the other side, must always be less than

$1/100$  of the voltage divider current in order to keep constant the gain of the PMTs respect to possible beam intensity variations. In order to fulfill this condition, the voltage divider impedance was lowered from  $5.65\text{ M}\Omega$  to  $1.80\text{ M}\Omega$ , while the power supply was fixed to a minimum value by measuring the FWHM resolution of the  $^{137}\text{Cs}$  gamma line as a function of the voltage supply: a value of about 1000 V, below which the resolution worses, was found on all PMTs.

## 2.2. Electronics

In fig. 2 the electronic scheme of the spectrometer is shown. The anode signals from the BGO crystals were summed cylinder by cylinder and all cylinders were summed together in an ORTEC Dual Mixer AN308/NL. In order to reduce pile-up effects, clipping of the anode signal at  $\Delta t = 170$  ns was also performed by reflecting the summed anode signal into a  $50\ \Omega$  coaxial cable. All the NaI anodes were summed together and clipped ( $\Delta t = 90$  ns) in a similar way and a threshold was set on the resulting analog signal to get anticoincidence inhibit for the charge ADC fed by the BGO anodes.

For both BGO and NaI crystals RC-shaping, which warrants a better rise time uniformity over a wide dynamical range, was performed by a timing filter (ORTEC 434), while a constant fraction discriminator provided a timing pulse.

Each PMT of both BGO and NaI crystals provided also a dynode signal that were all summed together, separately for BGO and NaI PMTs, to provide two pulses which could be used for linear analysis alternatively or in conjunction with charge analysis, being less affected by disturbances travelling on the coaxial cables. Before to be fed to the V-ADC, these summed dynode signals were shaped and amplified by a Timing Filter (ORTEC 454).

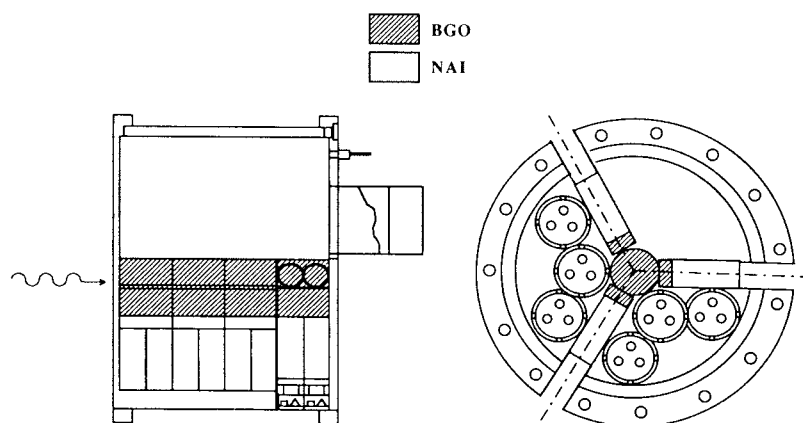


Fig. 1. Side and rear view of the BGO and NaI photon spectrometer, showing the crystals and phototubes.

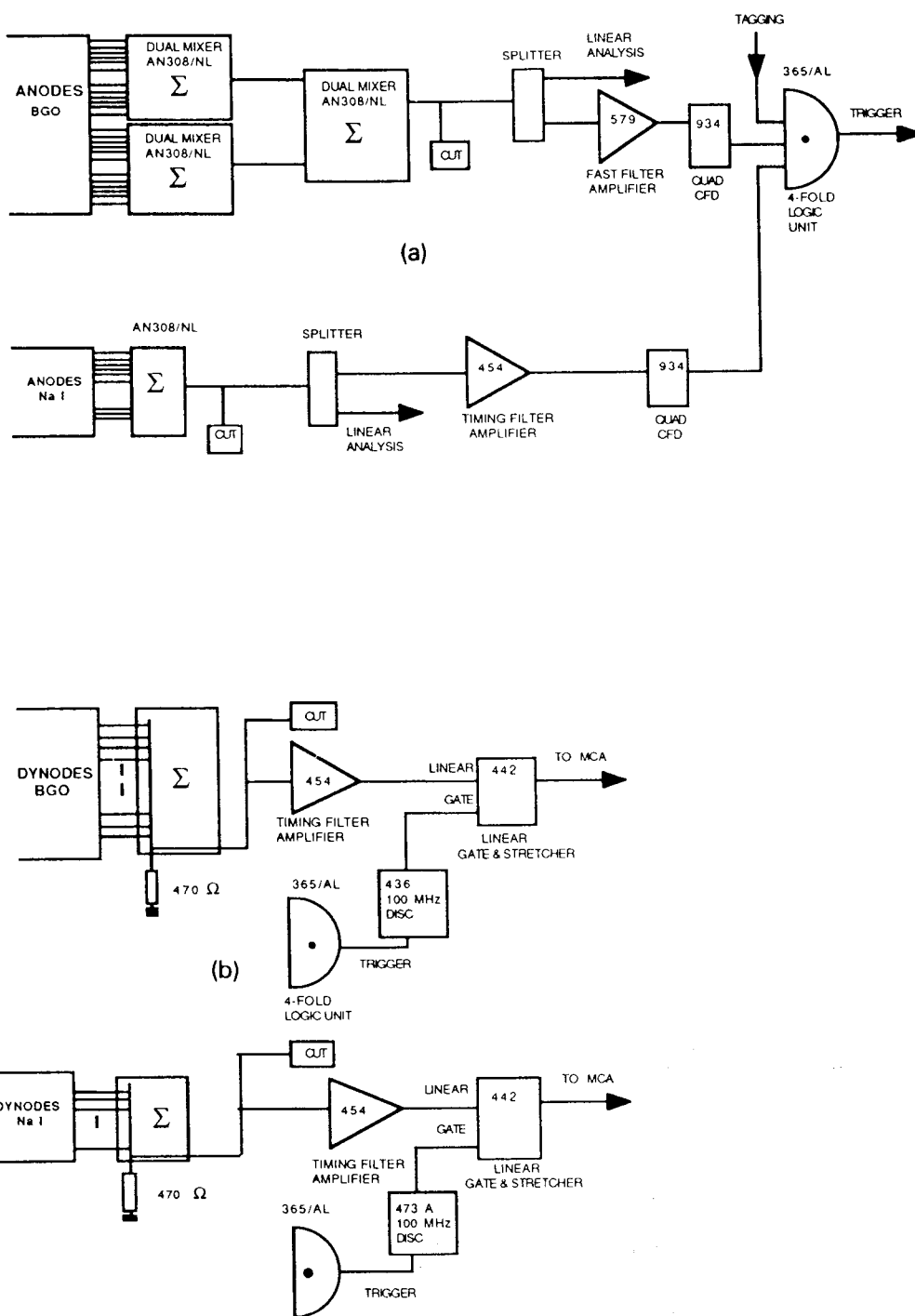


Fig. 2. Block diagram for the electronics used to process the analog and logic signals from the photon spectrometer.

### 2.3. Calibration

Both in BGO and NaI crystals, the intercalibration of the PMTs was done using  $\gamma$  radioactive sources (as said above) and cosmic rays. For this latter calibration

two configurations were used. For the BGO crystals, the spectrometer was vertically positioned and energy losses in each crystal were detected only for events crossing all the four cylinders: this procedure of calibration has been found particularly suitable due to the

longitudinal and radially isotropic energy release, simulating to an extent greater than the point-like  $\gamma$  sources the photon electromagnetic showers. For the NaI crystals, the spectrometer was horizontally positioned, and the NaI energy losses on each sector in coincidence with the BGO cylinders were detected: due to the cylindrical symmetry, it is possible in this way to directly compare the response of NaI crystals to each other.

Moreover, light emitting diodes (LED) were mounted on each crystal: three on each BGO sector and one on each NaI sector. A precision pulse generator supplied the LEDs at a programmed rate with a couple of pulses of different amplitude: the monitoring of these two output amplitudes, as well the input ones, ensured a fine control of possible variations of the analog readout.

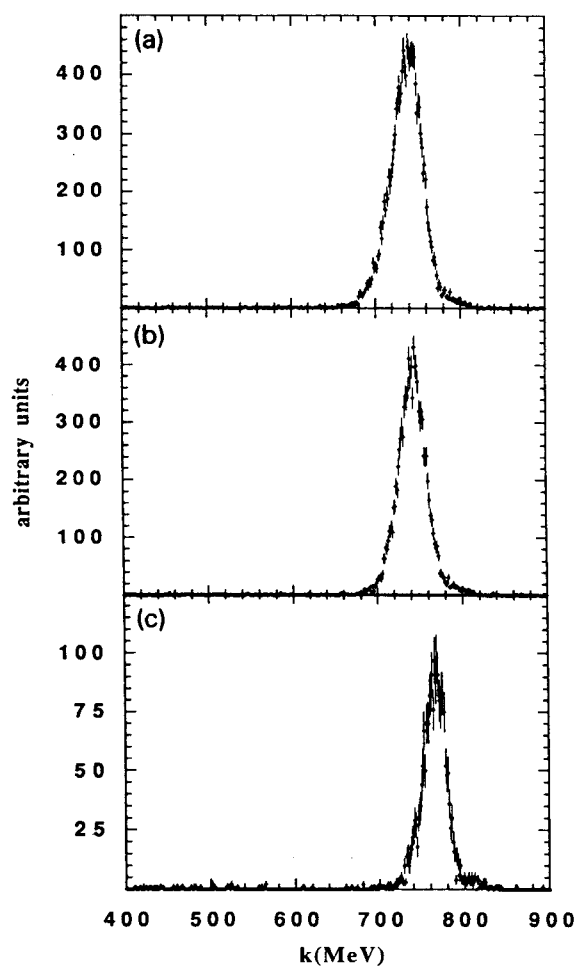


Fig. 3. Response function of the BGO crystals to tagged photons of energy  $750 \text{ MeV} \pm 1.5\%$ : (a) without NaI in anticoincidence; with a NaI anticoincidence thresholds of  $\approx 30 \text{ MeV}$  (b), and  $\approx 10 \text{ MeV}$  (c), respectively.

#### 2.4. Temperature control

The BGO crystals are sensitive to temperature variations; in the range from  $-5$  to  $35^\circ\text{C}$ , the emission light yield varies with a constant gradient of  $-1.2\%$  per centigrade degree [7]. To overcome this problem, the BGO crystals were thermostated within  $0.2^\circ\text{C}$  by a refrigerating liquid flowing inside a thin copper tube wound around the crystals. Moreover, the experimental hall in which the spectrometer was held was air conditioned.

We tested the stability of the spectrometer read out continuously measuring the LED light peak as well the  $\gamma$  source lines for several days keeping the crystal at constant temperature: gain variations less than  $1-2\%$  were observed.

### 3. Detector performances and results

The spectrometer is used at Frascati on the so called Jet Target tagged photon beam. This beam is produced by the bremsstrahlung on an argon cluster-beam of the electrons circulating into the ADONE storage ring. The cluster-beam is placed in the straight section n.5 between consecutive lattice elements of the ring: the recoil electrons are momentum analyzed by the next dipole magnet and detected by two arrays of scintillation counters in coincidence (39 counters in each array), placed between the ring vacuum pipe and the dipole magnet flux return yoke. The scintillators define 76 energy channels and have different sizes to give the same photon energy resolution for a given machine energy setting  $E_0$ , specifically: about  $1\%$  at  $E_0 = 1.5 \text{ GeV}$  and about  $2.7\%$  at  $E_0 = 0.5 \text{ GeV}$  over the whole tagging range  $E_\gamma = (0.4-0.8)E_0$  [4]. For an average circulating current in ADONE of  $\approx 60 \text{ mA}$  and an argon cluster-beam density of  $\approx 5 \text{ ng/cm}^2$ , the intensity of the photon beam in the tagging range is  $\approx 6 \times 10^7 \text{ } \gamma/\text{s}$ , that is about  $7.5 \times 10^5 \text{ } \gamma/\text{s}$  per energy channel [3,4].

In order to determine the tagging efficiency of the tagger, the BGO spectrometer was placed directly on the photon beam: since this detector has essentially  $100\%$  efficiency for detecting photons in the range of interest, a measurement of the ratio of photons detected by the BGO in coincidence with signals from each of the tagging electron counters to the total number of events detected by this counter determines the tagging efficiency. The incident photon beam was collimated to  $1 \text{ cm}$  diameter by two lead collimators several meter before of the BGO detector. Moreover, its intensity had to be reduced by four order of magnitude respect to the maximum flux (about  $10^8 \text{ } \gamma/\text{s}$  in the full energy range) in order to perform this measurement since the BGO spectrometer cannot correctly

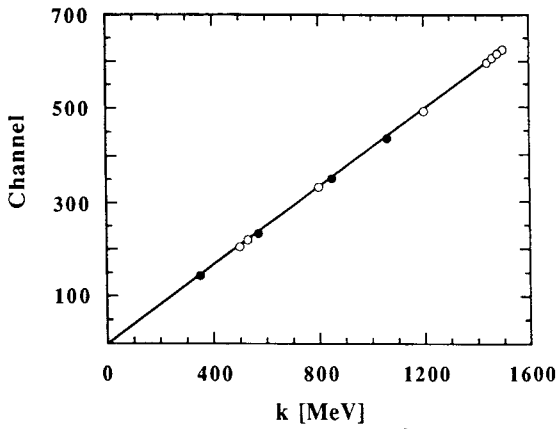


Fig. 4. Relation among channel position in the ADC spectrum of the BGO signals and the corresponding photon energies; open circles: head of the bremsstrahlung spectra; full circles: tagging channels.

work at high photon fluxes, being sensitive to the entire bremsstrahlung spectrum.

The coincidence between a given tagging channel and the BGO spectrometer signal readout gives also a powerful energy calibration method to determine the spectrometer response function to incident monochromatic photons. In fig. 3 are shown the BGO response functions at  $E_0 = 1.5$  GeV, measured in coincidence with the tagging channel n.49 defining a photon energy  $E_\gamma = 0.75$  GeV not using (fig. 3a) and using the NaI anticoincidence to reject the incompletely contained shower for two different setting of the anticoincidence threshold:  $\approx 30$  MeV, (fig. 3b), and  $\approx 10$  MeV (fig. 3c). As it is seen the energy resolution greatly im-

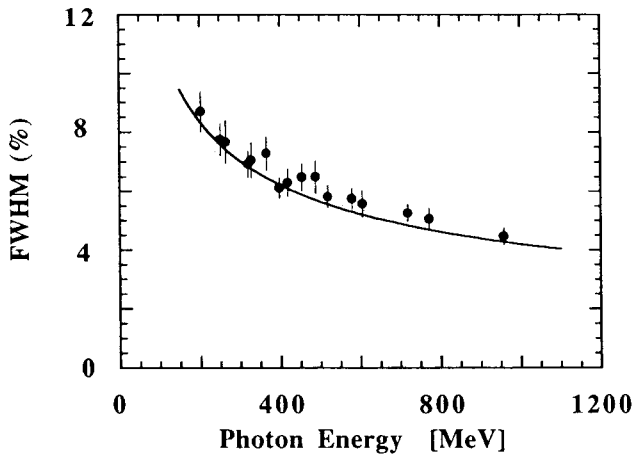


Fig. 5. Energy resolution (FWHM) of the BGO spectrometer versus photon energy; the full points are experimental results; the full line is the result of a Monte Carlo simulation of the detector response using the code GEANT 3.

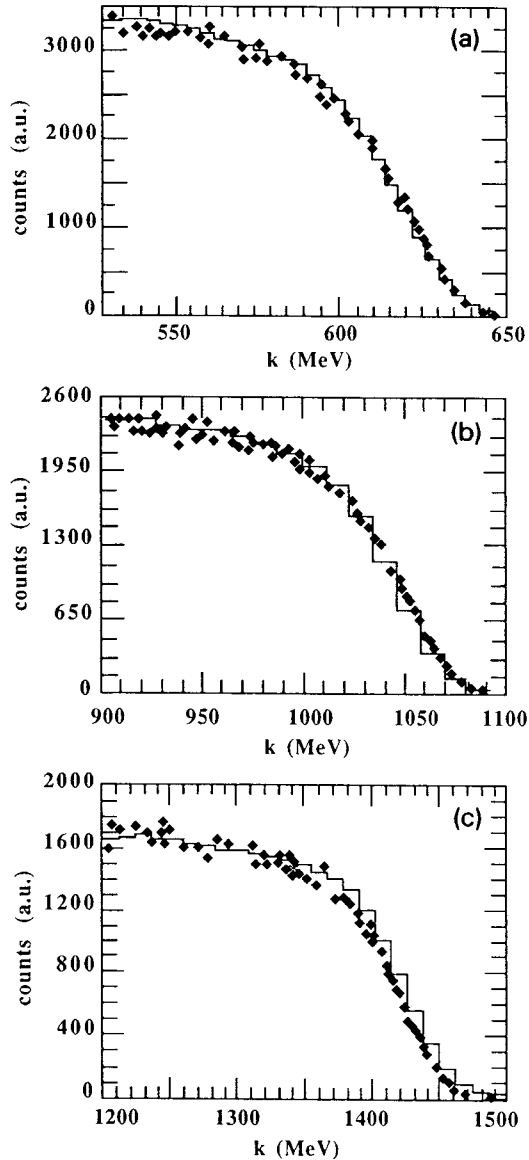


Fig. 6. High energy part of the bremsstrahlung spectra for electron energies of 650 MeV, 1100 MeV and 1500 MeV, calculated (histograms) and measured (full diamonds) by the BGO spectrometer. The calculated spectra have been convoluted with a 3% FWHM Gaussian response function to take into account such effects as crystals inhomogeneity and slightly different calibration between the four BGO crystals.

proves, passing from 5.7% to 3.5%; however, the cost of this improved resolution is a reduction in efficiency.

The linearity of the spectrometer response as a function of the photon energy was checked between 0.3 GeV up to 1.5 GeV by measuring the position of the head of the bremsstrahlung spectra at different electron energies. In the figure are also given the energy of peaks from the coincidence with different tagging

channels. As it is shown in fig. 4 a linear behaviour at a level better than 1% was found.

The BGO energy resolution is the result of a convolution of the intrinsic BGO statistical resolution with contributions from the tagging channel resolution, the lateral energy escapes and the PMT's response. In fig. 5 the experimental energy resolution (FWHM) simultaneously measured in coincidence with different tagging channels for different electron energy settings ( $E_0 = 0.37, 0.8, 1.1$  and  $1.5$  GeV) are given. This energy resolution width roughly scales as  $E_\gamma^{-0.35}$ , an intermediate value between the pure statistical behavior,  $E_\gamma^{-0.5}$ , and the  $E_\gamma^{-0.25}$  energy dependence already observed in previous works [8,9]. The continuous curve in fig. 4 (which scales as  $E_\gamma^{-0.43}$ ) is the result of a Monte Carlo shower simulation using the GEANT 3 code [10] which includes the geometrical characteristics of the BGO photon spectrometer and the tagging resolution: the observed discrepancy between measured and calculated energy resolution, more evident at higher energies, may be ascribed to the crystal's inhomogeneity, as well to a slightly different energy calibration of the four BGO crystals.

For the measurement of the total photoabsorption cross section on Be and C targets we used the transmission technique [6], which consists in measuring the total attenuation cross section and subtracting the calculated atomic absorption cross section. Photons crossed the absorption target put inside a dipole magnet and were detected, about 13 m downstream, by the BGO spectrometer. This lay-out afforded good rejection of the forward components of the electromagnetic showers created in the absorber. Experimentally, we measured with high accuracy the bremsstrahlung spectra of photons reaching the BGO spectrometer respectively with and without the absorbing target on the beam. To normalize the target-in and target-out photon spectra, we used a photon monitor permanently inserted on the photon beam before the target position. Running conditions, such as jet thickness and electron current, were adjusted to maintain constant ( $\approx 2$  kHz) the BGO rates with target-in and target-out, and to keep stable within 0.8% the response of the BGO spectrometer.

Measurements were carried out at several electron beam energies. As an example, in fig. 6 are quoted the higher energy part of the bremsstrahlung spectra measured by the BGO spectrometer at the electron energies  $E_0 = 0.65, 1.1$  and  $1.5$  GeV together with the Monte Carlo estimates. Experimental conditions were: Argon radiator of  $0.05\text{--}0.1$  ng/cm<sup>2</sup>, a photon collection angle between 0 and  $10^{-4}$  rad, and the photonuclear absorption target out of the beam. The input bremsstrahlung spectra for the Monte Carlo were taken from the recent paper of Seitzer and Berger [11], who

derived a comprehensive set of cross section (differential in the energy of the emitted photon) through the synthesis of various theoretical results. As it can be seen, the agreement between data and calculations is rather good.

#### 4. Conclusions

We have studied the behaviour of a  $32\text{ cm} \times 9.5\text{ cm}$  BGO, surrounded by NaI crystals, to the Frascati Jet Target tagged photons from 0.2 to 1.2 GeV. Measurements made at these energies agree well with calculations of the GEANT3 electromagnetic showering code. The results indicate that the spectrometer can be used as a reliable monitor for energy calibration, efficiency measurements and absolute normalization in photonuclear experiments at intermediate photon energies.

#### Acknowledgements

The authors want to express their acknowledgements to A. Rottura for the LED installation on the BGO and NaI crystals and the construction of the temperature control system.

#### References

- [1] J.A. Bakken et al., Nucl. Instr. and Meth. A254 (1987) 535.
- [2] M. Anghinolfi et al., Frascati Internal Report, LNF-90/084 (R) (1990).
- [3] M. Taiuti et al., Nucl. Instr. and Meth. A297 (1990) 354.
- [4] E. De Sanctis et al., Proc. Terzo Convegno su Problemi di Fisica Nucleare Teorica, Cortona October 16–18 1989, eds. L. Bracci et al. (ETS Editrice Pisa) p. 75.
- [5] N. Bianchi et al., Nucl. Instr. and Meth., this issue A317 (1992) 434.
- [6] M. Anghinolfi et al., Proc. 5th Workshop on Perspectives in Nuclear Physics at Intermediate Energies, Trieste May 6–10, 1991, eds. S. Boffi, P. Ciofi degli Atti and M. Giannini (World Scientific Publishing Co., Singapore) in press; and M. Anghinolfi et al., Proc. VIII Seminar on Electromagnetic Interactions of Nuclei at Low and Medium Energies, Moscow, 2–5 December 1991, eds. R. Eramzhyan and V. Nedorezov, in press.
- [7] A. Zucchiatti, C. Bernini, G. Gervino and A. Rottura, Nucl. Instr. and Meth. A281 (1989) 341.
- [8] D.J. Wagenaar et al., Nucl. Instr. and Meth. A234 (1985) 109.
- [9] L. Adiels et al., Nucl. Instr. and Meth. A244 (1986) 380.
- [10] R. Brun et al., CERN, Data Handling Division DD/EE/84-1, September 1987.
- [11] S.M. Seitzer and M.J. Berger, At. Data Nucl. Data Tables 35 (3) (1986).